Core-defect reduction in ZnO nanorods by cobalt incorporation

Adrien Savoyant, H Alnoor, O. Pilone, O Nur, M Willander

Core-defect reduction in ZnO nanorods by cobalt incorporation

A. Savoyant,[1] H. Alnoor,[2] O. Pilone,[1] O. Nur,[2] and M. Willander[2]

[1]*IM2NP, CNRS UMR 7334, FST, Aix-Marseille Université, F-13397 Marseille Cedex 20, France*
[2]*Department of Science and Technology (ITN), campus Norkköping, Linköping University, SE-601 74 Norrköping, Sweden*

Zinc oxide (ZnO) nanorods grown by the low-temperature (90°C) aqueous chemical method with different cobalt concentration within the synthesis solution (from 0 % to 15 %), are studied by electron paramagnetic resonance (EPR), just above the liquid helium temperature. The anisotropic spectra of substitutional Co^{2+} reveal a high crystalline quality and orientation of the NRs, as well as the probable presence of a secondary disordered phase of ZnO:Co. The analysis of the EPR spectra indicates that the disappearance of the paramagnetic native core-defect (CD) at $g \sim 1.96$ is correlated with the apparition of the Co^{2+} ions lines, suggesting a gradual neutralization of the former by the latter. We show that only a little amount of cobalt in the synthesis solution (about 0.2 %) is necessary to suppress almost all these paramagnetic CDs. This gives insight in the experimentally observed improvement of the crystal quality of diluted ZnO:Co nanorods, as well as into the control of paramagnetic defects in ZnO nanostructures.

PACS numbers: 61.46.Hk, 61.72.uj, 75.75.Cd, 76.30.Fc

I. INTRODUCTION

Zinc oxide (ZnO) micro and nanostructures are highly interesting materials since they offer a wide variety of morphologies[1] (rods, dots, rings, etc.), tunable semiconducting and optical properties when doped[2,3], are health friendly and of low fabrication cost[4]. In particular, ZnO nanorods (NRs) are the focus of great attention because their one-dimensional character allows researchers to obtain coherent orientation of them, while keeping high surface area/volume ratio and interesting piezoelectric properties.
Currently, ZnO NRs are involved in many functional electronic devices such as light emitting diode[5], fast UV detectors and pressure sensors[6]. In these applications, native (intrinsic) or intentionally introduced (extrinsic) defects play a major role. For instance, in all luminescence phenomena, intrinsic and extrinsic defects in ZnO are involved as steps in the excitation and/or recombination paths, hence influencing the absorbed or emitted light properties (photon energy, relaxation time, etc.). On the other hand, electrical conduction in semiconductors is entirely driven by the ability of these defects to provide delocalized electrons (holes) in the conduction (valence) bands. Consequently, the knowledge and control of intrinsic and extrinsic defects, as well as the relation between both, are key issues for the electronic and optical optimization of ZnO nanostructures.

The case of paramagnetic defects is of particular interest because, when subjected to an external applied magnetic field, a majority of them (depending on temperature) have up (or down) spin projection, which then restricts the possible recombination paths *via* these polarized defects to those allowed by the Pauli exclusion principle. Regarding these paramagnetic defects, electron paramagnetic resonance (EPR) is a precious tool to characterize them and to study their occurrence as a function of the various synthesis parameters (synthesis temperature, stirring time, dopant, etc.). Simultaneously, EPR spectra can give information about the spin environment, the crystal quality at the atomic scale, and the macroscopic ordering. However, applying EPR spectroscopy on paramagnetic nanostructures is difficult, mainly because of the low amount of resonating centers and the large spin relaxation. Moreover, as most of the studies deal with non-oriented nanoparticles, information on magnetic anisotropy is often lost[7–9].
Nevertheless, in a previous study[11] based on EPR measurement of well-oriented ZnO:Co NRs, we have successfully used the Co^{2+} signal to prove the incorporation of these ions in well-oriented crystalline NRs phase, and have suggested that the drastic reduction of the intrinsic core defects (CD) at $g \sim 1.96$ of ZnO nanostructures observed in Co-doped samples was related to this cobalt incorporation. The fine structure and magnetic anisotropy of the $g \sim 1.96$ signal has been in addition determined.

In this work, by a systematic examination of the EPR spectra of ZnO:Co NRs grown with varying the cobalt concentration in the synthesis solution, from 0 % to 15 %, we prove that the apparition of the substitutional Co^{2+} signal is correlated with the disappearing of the paramagnetic CD signal at $g \sim 1.96$. The analysis of the Co^{2+} signal brings information about the ordered phase of NRs and suggests the presence of an additional disordered phase of the same ZnO:Co system. In addition to give some insight into the observed augmented crystal quality of low Co-doped ZnO

NRs[12], this work opens the path to accurately control the number of these paramagnetic CDs with relatively small amount of dopant incorporation.

II. METHODS

The samples under study are made of ZnO:Co NRs of length and diameter 3.5 μm and 200 nm, respectively, grown on a ZnO nanoparticles (20-50 nm of diameter) seed layer, deposited on a 3mm×3mm×0.43mm sapphire substrate. These samples, with different Co concentration within the synthesis solution, were grown by the low-temperature (90°C) chemical aqueous method described in Ref. 11. Scanning Electron Microscopy (SEM) images of 0.2, 2, 10 and 15 % samples are shown in Fig. 1.
The EPR measurements were performed on a conventional Bruker ELEXSYS continuous wave spectrometer operating at X-band ($\nu = 9.38$ GHz) using a standard TE_{102} mode cavity. The orientation of the samples was insured by manual goniometer with a precision of 0.5°, and allow to set the angle between the applied magnetic field B and the c-axis of the wurtzite ZnO nanocrystals, parallel to the NRs and perpendicular to the substrate surface. Due to the low Co and CD absolute number, signals have been accumulated to increase the signal/noise ratio. All measurements have been performed at a temperature of 6 K. As no reference line was added to the spectra, the exact magnetic field is not known with precision lower than 2-4 G, and the absolute g-factor values may have to be slightly corrected by an amount of 0.002.

III. RESULTS AND DISCUSSION

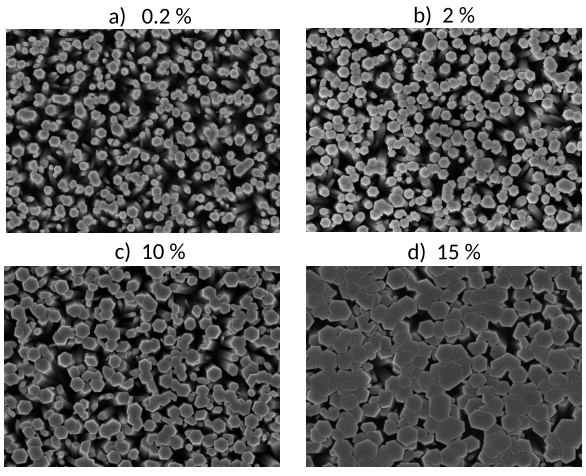

Figure 1: (color online) Top-view of the 0.2, 2, 10 and 15 % samples recorded by SEM. All images have 5×6 μm dimensions.

The scope of this work is to compare the EPR line's intensity of the substitutional Co^{2+} ions to that of the CD when the Co concentration within the synthesis solution is varied, in order to compare the respective number of these extrinsic and intrinsic defects. The EPR intensity of a given line can be expressed as $I = K.W.f(T).N$, where K is a constant depending on experimental condition, W is the transition probability, $f(T)$ is a temperature-dependent function, and N is the number of resonating spins (see Ref. 11). By recording all spectra at the same temperature (6 K), scaled to the same experimental conditions (10 dB attenuation, 5 G modualation), and assuming that transition probabilities are of the same order ($W_{co} \sim W_{cd}$), the ratio I_{co}/I_{cd} will give the ratio of extrinsic/intrinsic defects numbers. Even if these transition probabilities are substantially different, as they are regarded as constant quantities, the evolution of the intensities ratio will reflect the evolution of the defects numbers ratio.
In order to determine the EPR intensities, two main methods are usually employed: (1) the double integration procedure or (2) the fitting of each spectrum by an appropriate simulation. However, the first method demands high signal/noise ratio with negligible baseline, while the latter requires precise and certain models for each lines. Both of these methods are inappropriate in our case, firstly because the recorded signals are very noisy due to the low resonant centers quantity in NRs and, secondly, because some of the lines are a superposition of several lines (see below), which makes the simulation difficult by increasing the number of adjustable parameters. In addition to these constraints, the chosen method must be identically used for each line. We then adopt a third solution, which is based on roughly estimate a line's intensity by multiplying its width by its peak-to-peak height. This method is only rigorously valid for a single 1/2 spin line, symmetric and without any substructure. Nevertheless, in the following, all intensities will be calculated by this third method, and it will be assumed to give reasonable estimation for the relative intensities and their evolution.

The typical EPR spectra of the samples under study are shown in Fig. 2. The substitutional Co^{2+} ions give highly anisotropic signal, characterized by an eight-lines structure at $B \sim 300$ mT for $\theta = 0°$ (Fig. 2-c) and a broad asymmetric single line at $B \sim 150$ mT for $\theta = 90°$ (Fig. 2-b), as previously observed in similar samples[11]. When the Co concentration within the synthesis solution is decreased, the Co^{2+} signal decreases (Fig. 2-a) while the CD signal begins to appear at $B \sim 346$ mT ($g \sim 1.96$). This latter reaches a maximum intensity for pure ZnO NRs. In some of the samples

(10 % and 0.5 %), point defects in the crystalline sapphire substrate give line very closed to the CD signal for the $\theta = 0°$ orientation (see Fig. 2). Fortunately, this sapphire defect (SD) line cannot be mistaken with the CD one, because of its great and known anisotropy: rotating the sample by 90° with respect to the magnetic field shifts the SD line to $B \sim 175$ mT field, while the CD line practically does not move (Fig. 2). For this reason, the $\theta = 90°$ orientation is preferable in order to study the CD line's intensity without signal interference. In the following, we begin by analyzing the Co-related signal and discuss some of its characteristics and, after that, we focus on the CD signal.

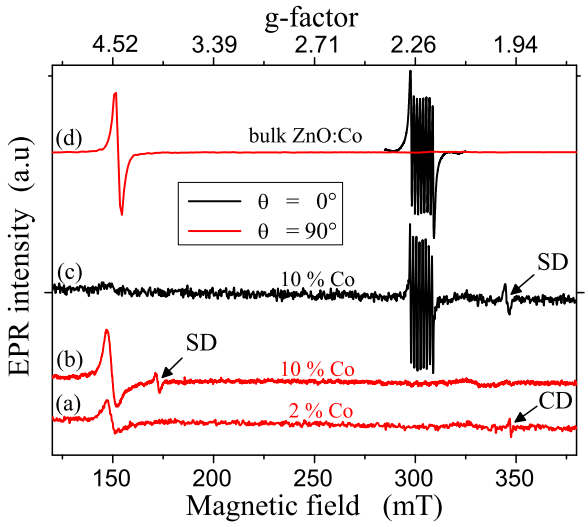

Figure 2: (colour online) EPR spectra of 10 and 2 % Co-doped samples, showing the anisotropy of the Co^{2+} signal, recorded at $T = 6$ K. Sample holder (SH), sapphire defect (SD) and core defect (CD) lines are indicated.

The Co^{2+} spectra for both orientations, and for each sample, are all shown in Fig. 3. Their intensities, line width and position (g-factor) are reported in Tab. I. Regarding these Co^{2+} spectra, two interesting facts have to be pointed out. Firstly, and contrary to what can be expected, the $I_{co}^{\parallel}/I_{co}^{\perp}$ ratio is not constant in each sample, and, secondly, the Co^{2+} line at 150 mT (for $\theta = 90°$) displays a pronounced asymmetry (positive and negative parts are not equal). We will see that these two points are likely to reflect the presence of a secondary, disordered, phase of ZnO:Co.

Regarding the first point, although the number of substitutional Co^{2+} varies from one sample to another, if these ions are sufficiently diluted in the same ordered ZnO matrix, the $I_{co}^{\parallel}/I_{co}^{\perp}$ must be constant. As it is not the case in our samples, it is interesting to evaluate this ratio for a perfectly crystalline ZnO:Co system. We do that by estimating the $I_{co}^{\parallel}/I_{co}^{\perp}$ ratio with the same method in single crystalline ZnO:Co microwire grown by optical furnace method (see Fig. 2-d), and find a ratio of $I_{co}^{\parallel}/I_{co}^{\perp} = 1.3$. This value has to be seen as a lower limit because the concerned microwire has been proved to be inhomogeneous in Co doping[13], so that several Co^{2+} pairs contribute to the 150 mT line at $\theta = 90°$ leading to an overestimation of $I_{co}^{\perp}$. Compared to this value, the estimated ratio in all our samples is systematically lower: 0, 0.85, 0.96, and 0.55 for the 0.5 %, 2 %, 10 %, and 15 %, respectively. This variation can be explained if, in addition to the well-orientated ZnO:Co NRs giving rise to $I_{\parallel}$ and $I_{\perp}$, there exists another phase of the same ZnO:Co system which only contributes to $I_{\perp}$ by augmenting its intensity and breaking the line symmetry. The variation of the $I_{co}^{\parallel}/I_{co}^{\perp}$ ratio would then reflects the variation in the relative proportion of the two phases.

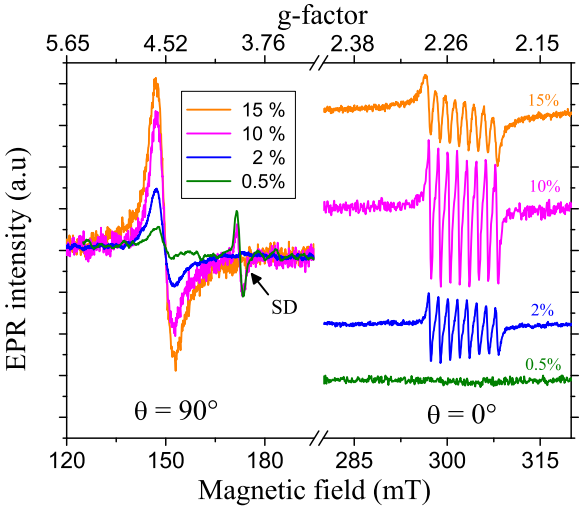

Figure 3: (color online) Evolution of the Co^{2+} signal with the cobalt concentration within the synthesis solution, for both orientation, recorded at $T = 6$ K. Spectra for $\theta = 0°$ are divided by 3.

The other mentioned point (asymmetry) tends to support and to specify this hypothesis. Indeed, while the eight-lines structure recorded for the $\theta = 0°$ orientation clearly arise from substitutional Co^{2+} ions in orientated crystalline ZnO NRs, this is not the case for the broad line at $B \sim 150$ mT. Simulation and experiment on bulk ZnO:Co (Fig. 2-d) show that the asymmetry and the relative intensity of this latter line are not compatible with the simple rotation of the orientated ZnO:Co NRs, which would give a symmetric line of weaker intensity. Keeping in mind that the EPR lines are derivative of the absorption lines, the observed asymmetry is the consequence of a wide distribution in some of the Co^{2+} parameters, which is most likely to be an angle distribution, indeed very closed to that of a powder spectra. Such a powder spectrum would precisely gives an isotropic and asymmetric line at 150 mT and, actually, a

trace of it can be seen in the spectrum of Fig. 2-c (10 %, 0°), unfortunately not sufficiently resolved. We are then led to conclude that, in addition to the well-orientated ZnO:Co NRs phase, there exists a little disordered phase of the same system which contributes to the 150 mT Co^{2+} line. The better evidence for that is the 0.2 % sample spectra, in which only the broad line at 150 mT is visible (see Fig. 3). The nature of this disordered ZnO:Co phase has not been elucidated, but is likely to be a set of ZnO:Co nanoparticles or badly oriented NRs distributed within the sample. To accurately quantify the relative amount of these two phases would require precise simulations of better-resolved spectra, recorded with additional intermediate orientations. Such simulations would be difficult to perform because of the anisotropy of the line width (not taken into account in common powder simulations) and of the required knowledge of the perpendicular hyperfine constant $A_\perp$ which, moreover, may be different in the ordered and disordered phases.

As a consequence, we state that while the Co intensity at $\theta = 0°$ is proportional to the number of Co^{2+} ions in the well-orientated phase, the Co intensity at $\theta = 90°$ is proportional to the whole number of Co^{2+}, within the ordered and disordered phases. Then, for the aim of comparing the total number of incorporated Co^{2+} ions to the number of CDs, we will use the cobalt intensity recorded at $\theta = 90°$.

Table I: Evolution of EPR lines parameters with increasing concentration. All line widths are in mT and the intensities are in arbitrary unit scaled so that it is 100 for the CD line of pure ZnO NRs.

	Co^{2+}						CD		
x	$g_{co}^{\perp}$	$w_{co}^{\perp}$	$I_{co}^{\perp}$	$g_{co}^{\parallel}$	$w_{co}^{\parallel}$	$I_{co}^{\parallel}$	$g_{cd}^{\perp}$	$w_{cd}^{\perp}$	$I_{cd}^{\perp}$
0	–	–	0	–	–	0	1.955	0.09	100
0.2	–	–	0	–	–	0	1.958	0.67	5.1
0.5	2.258	4.3	5	–	–	0	1.957	0.53	2.3
2	2.259	5.3	20	2.239	0.38	17	1.956	0.64	1.6
10	2.261	5.3	45	2.239	0.40	43	1.955	1.8	0.6
15	2.258	5.6	58	2.241	0.75	32	–	–	0

The examination of the intensities evolution indicates that the total number of incorporated Co^{2+} ions ($\propto I_{co}^{\perp}$) continuously increases, while their number in the ordered phase ($\propto I_{co}^{\parallel}$) reaches a maximum for 10 % of Co in the synthesis solution. This is consistent with the previous study on ZnO:Co NRs grown with the similar low-temperature method, which has stated that the maximum number of incorporated Co^{2+} arise at about 1 % of cobalt in the synthesis solution, and that above this value the crystal quality is degraded[12]. This may be understood by noting that ZnO:Co is not an equilibrated thermodynamic system, so that low-temperature growth method can only incorporate a small amount of Co in the ZnO matrix. Indeed, the 10 % sample has also the closest $I_{co}^{\parallel}/I_{co}^{\perp}$ ratio (0.96) to the single crystal one (1.3), thus appearing as a better ordered and crystalline sample. This is consistent with the SEM images of the different samples (Fig. 1), which show that the 10 % sample has the highest Co concentration while preserving the NRs integrity.

Regarding the evolution of the other Co^{2+} parameters, we note that the parallel hyperfine constant ($A_\parallel$), defined by the spacing between two hyperfine lines, is the same in all samples where it can be detected ($16\times10^{-4}\text{cm}^{-1}$), and is almost exactly that of the bulk case, thus indicating a high crystallinity of the ordered phase. The perpendicular hyperfine constant ($A_\perp$) is not resolved in the 150 mT broad line because it is lower than the perpendicular line width.

For the g-factors, we recall that the position of the 150 mT broad line gives an effective value, $g_{eff}^{\perp} = 2g_{co}^{\perp}$ (see Ref. 11). The $g_{co}^{\perp}$ and $g_{co}^{\parallel}$ are closed to their bulk values (2.279, 2.243), but due to the asymmetry of the 150 mT line, there is a notable uncertainty in the $g_{co}^{\perp}$ value and conclusions about a variation of the anisotropy are difficult to draw.

The perpendicular line width ($w_{co}^{\perp}$) is practically constant and does not bring much information since it results from a lines superposition and unresolved hyperfine coupling ($A_\perp$). On the contrary, the augmentation of the parallel line width ($w_{co}^{\parallel}$) indicates a continuous increase in the Co^{2+} concentration within the ordered phase, due to dipolar broadening. By comparing the 10 and 15 % sample, we see that the latter has a lower number of orientated Co^{2+}, which are however more concentrated: this can be interpreted as a reduction of the ordered phase volume in the 15 % sample, consistent with its lowest $I_{co}^{\parallel}/I_{co}^{\perp}$ ratio (0.55) and SEM imaging (Fig. 1).

We now turn to the study of the intrinsic defects signal, which gives lines around $g \sim 1.96$. Previously, several defect signals have been detected close to this value, both in bulk and nano-sized ZnO materials[14–17]. Their identification still remains controversial but two main assignments are usually made: (1) a single-ionized zinc interstitial (Zn_i^+) at $g_\perp = 1.9595$ and $g_\parallel = 1.9605$[17,18], and (2) the so-called D* center at $g_\perp = 1.9605$ and $g_\parallel = 1.9565$[19,20]. Besides, a $g \sim 1.96$ signal has been proved to decrease when reducing the ZnO nanoparticles size, thus being attributed to a shallow donor CD signal[21–23]. However, the nanoparticles not being oriented, the information on anisotropy is lost so that the signal may arise from defects mentioned in (1), (2), or both. On the contrary, when dealing with oriented nanos-

tructures, it is valuable to characterize the defects by the anisotropy (if any) of their g-factor components. Defining $\Delta g = g_\perp - g_\parallel$, the two above-mentioned defects have $\Delta g = -0.0010$ (easy-axis) and $\Delta g = +0.0040$ (easy-plane), respectively. The difference in the anisotropy type of these defects points to their different nature.

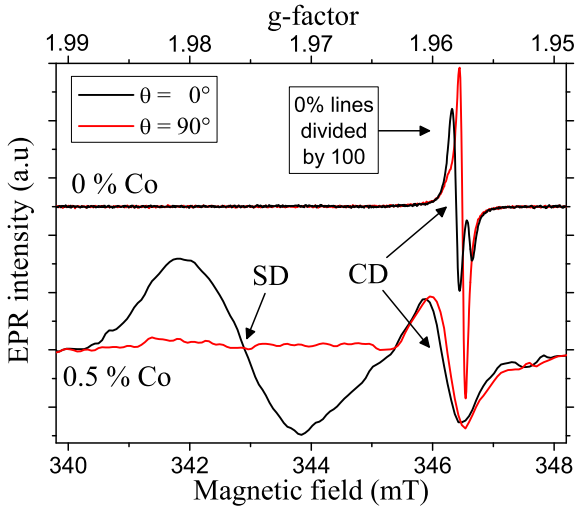

Figure 4: (colour online) Anisotropy of the EPR CD signal in pure (0 % Co) and Co-doped (0.5 %) samples, with respect to the magnetic field orientation, recorded at $T = 6$ K. Sapphire defect (SD) signal present in the 0.5 % sample is shown for the $\theta = 0^\circ$ orientation.

Regarding our samples, we first note that in all of them, excepting the $g \sim 1.96$ CD signal, no other defect or pollution-related lines are detected, pointing to the high crystal quality and purity of the NRs under investigation. The CD signal detected on the pure ZnO NRs (Fig. 4-top) is made of at least two closed lines, which collapse into a single asymmetric line for $\theta = 90^\circ$. Here, one of these observed lines appears to be almost isotropic, while the other one displays a slight easy-axis anisotropy signed by the displacement of the positive peak. This shift allows us to estimate Δg for the anisotropic line to be -0.0014, thus likely to be related to a Zn_i^+ defect ($\Delta g = -0.0010$) within the ordered phase of NRs. Regarding the isotropic line, although an isotropic defect cannot be excluded, it is likely to be related to the previously mentioned disordered phase. If so, the line may arise from a *powder* of the anisotropic defect, with slightly modified parameters: this could be the case for disordered ZnO:Co large nanoparticles or partially grown NRs.
We note that in a previous study on similar samples[11], we have observed a three-line structure at $g \sim 1.96$, denoting the presence of another kind of resonant center. This additional line displays an easy-axis anisotropy closed to that of the (probable) Zn_i^+ signal, so that it must arise from the ordered phase of NRs as well.
Concerning the intensities estimation, we keep the same simple method as before, which is better applied for the $\theta = 90^\circ$ CD spectra, when a single asymmetric line is present and the SD signal is shifted toward low field (Fig. 4). We then determine the g-factor ($g_{cd}^\perp$), line width ($w_{cd}^\perp$) and height, thus obtain the $I_{cd}^\perp$ intensity (Tab. I), proportional to the whole number of $g \sim 1.96$ CDs.

When a small amount of Co is introduced within the synthesis solution, the total CD signal is drastically reduced by a factor ∼20 in the 0.2 % sample, and a factor ∼50 in the 0.5 % sample (see Tab. I). In these Co-doped samples, the two-lines structure of the $\theta = 0^\circ$ orientation is not anymore visible and there only remains a broader line, whose asymmetry indicates an underlying structure (Fig. 4-bottom). This broad line displays an easy-axis anisotropy $\Delta g = -0.0012$, so that it is reasonably assumed to arise from the same anisotropic (probable Zn_i^+) defect present in the pure sample ($\Delta g = -0.0014$). The isotropic line of the pure ZnO NRs discussed above is likely to be responsible for the observed right shoulder of the reduced line. We note that the two lines (anisotropic and isotropic) of the pure ZnO NRs samples are similarly reduced in their intensity, and augmented in their line width. The line width augmentation is certainly due to the presence of polarized Co^{2+} ions which cause a dipolar broadening, but also an increased spin-spin relaxation due to the Co^{2+} open d-shell.

Regarding the evolution of the CD signal for $\theta = 90^\circ$, figure 5 clearly shows that the CD intensity (number) decreases with the increase of Co in the synthesis solution. However, the comparison of absolute intensity in different samples does not lead to significant information since the total number of the NRs may vary from a sample to another, mainly due to differences in the substrate coverage. Consequently, in order to indubitably correlate this decrease with the increase of total number of incorporated Co^{2+}, it is preferable to plot the CD's intensity ($I_{cd}^\perp$) with respect to the Co intensity at $\theta = 90^\circ$ ($I_{co}^\perp$), rather than with respect to the Co concentration within the synthesis solution. This has been done in the inset of Fig. 5, which clearly shows that the incorporation of Co^{2+} ions (in ordered and disordered phases) is accompanied by the progressive disappearance of the the CD signal. This anti-correlation does moreover follow qualitatively the Co content within the synthesis solution so that, for example, the 10 % sample has more incorporated Co and less CD than the 2 % sample.

To analyze this, three main explanations are pos-

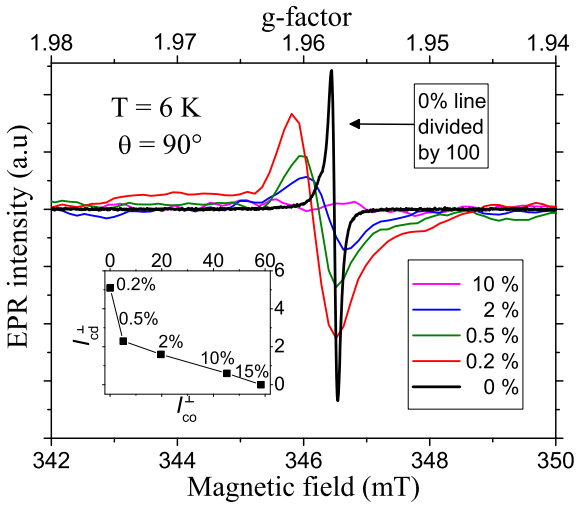

Figure 5: (color online) Evolution of the CD signal with the cobalt concentration within the synthesis solution. Line of the 0 % is divided by 100. The 15 % sample spectra is not shown for clarity (similar to the 10 % one). Inset shows $I^{\perp}_{cd}$ vs $I^{\perp}_{co}$.

sible: (1) the presence of cobalt in the synthesis solution may, in a way or another, simply inhibit the formation of this defect during the growth, (2) the paramagnetic incorporated Co^{2+} ions and CD may form a non-magnetic complex, which is then not detectable by EPR, or (3) another kind of non-magnetic incorporated cobalt may destroy the CD, for example by filling a vacancy. It has also been suggested that the disappearing of the $g \sim 1.96$ signal when transition metal ions are incorporated in ZnO is only due to a large broadening due to spin-spin relaxation with the 3d electrons[23]. However, it is difficult to imagine a Co^{2+} ion interacting so with a CD without being altered in its magnetic parameters, so that, as only Co^{2+} ions with bulk parameters are detected, this suggestion may be finally equivalent to the case (2). Indeed, the physics of ZnO intrinsic and extrinsic defects is so rich that many kinds of defects complexes are likely to occur. Consequently, at this stage, we cannot decide an exact answer for this question, in particular because the exact nature of the CD is not known with certainty. Further experimental and theoretical investigation have to be done. For instance, *ab initio* theoretical study of ZnO supercells containing various kind of paramagnetic defects (compatible with the slight easy-axis magnetic anisotropy observed in this work) and substitutional Co^{2+} ions in various relative positions would be able to give insight into these questions.

IV. CONCLUSION

We have detected the EPR signal of substitutional Co^{2+} ions in the ZnO matrix of NRs. The analysis of the anisotropic spectra indicates a high crystallinity of the NRs, which are moreover mostly well-oriented perpendicularly to the substrate surface. The line-shape analysis of the Co^{2+} signal reveals the probable presence of a secondary disordered phase of ZnO:Co.
Besides, the resolved anisotropy of the CD signal at $g \sim 1.96$ in pure NRs strongly suggests that this defect signal arises, at least partially, from the Zn_i^+ shallow donor.
By a systematic examination of the EPR spectra recorded just above liquid helium temperature on samples grown with varying cobalt concentration within the synthesis solution, we prove that the apparition of the cobalt signal is anti-correlated with that of the CD signal, thus suggesting a gradual neutralization of the CD by Co^{2+}.
On one hand, these results can explain the augmentation of the ZnO:Co NRs crystal quality observed in low Co-doped samples and, on the other hand, it will allow researchers to finely tune the number of the paramagnetic defects in ZnO nanostructures, as well as to give insight into the identification of the $g \sim 1.96$ signal.

V. ACKNOWLEDGEMENT

This work was supported by the NATO project Science for Peace (SfP) 984735, Novel nanostructures. A. Savoyant and O. Pilone acknowledge Sylvain Bertaina for useful discussion about EPR measurement.

[1] Z. L. Wang, *Mater. Sci. Eng.* R **64**, 33 (2009).
[2] D. J. Norris, A. L. Efros, and S. C. Erwin, *Science* **319**, 1776 (2017).
[3] J. D. Bryan, and D. R. Gamelin, *Prog. Inorg. Chem.* **54**, 47 (2005).
[4] G. C. Yi, C. Wang, and W. I. Park, *Semicond. Sci. Technol.* **20**, S22 (2005).
[5] M. Willander, O. Nur, Q. X. Zhao, L. L. Yang, M. Lorenz, B. Q. Cao, J. Zúñiga Pérez, C. Czekalla, G. Zimmermann, M. Grundmann, A. Bakin, A. Behrends, M. Al-Suleiman, A. El-Shaer, A. Che Mofor, B. Postels, A. Waag, N. Boukos, A. Travlos, H. S. Kwack, J. Guinard, and D. Le Si Dang, *Nanotechnology* **20**, 332001 (2009).
[6] Chey, C. O., Liu, X., Alnoor, H., Nur, O. and Willander, M. (2015), *Phys. Status Solidi* RRL, 9: 87−91.
[7] L. B. Duan, W. G. Chu, J. yu, Y. C. Wang, L. N.

Zhang, G. Y. Liu, J. K. Liang, and G. H. Rao, *J. Magn. Magn. Mater.* **320** 1573 (2008).
[8] P. Lommens, K. Lambert, F. Loncke, D. De Muynck, T. Balkan, F. Vanhaecke, H. Vrielinck, F. Callens, and Z. Hens, *ChemPhysChem* **9**, 484 (2008).
[9] S. Kumar, T. K. Song, S. Gautam, K. H. Chae, S. S. Kim, and K. W. Jang, *Mat. Res. Bull.* **66**, 76 (2015).
[10] T. Ruf, S. Repp, J. Urban, R. Thomann, and E. Erdem, *J. Nanopart. Res.* **18**, 109 (2016).
[11] A. Savoyant, H. Alnoor, S. Bertaina, O. Nur, andM. Willander, *Nanotechnology* **28**, 035705 (2017).
[12] C.-W. Liu, S.-J. Chang, S. Brahma, C.-H. Hsiao, F. M. Chang, P. H. Wang, and K.-Y. Lo, J. Appl. Phys. **117**, 084315 (2015).
[13] A. Savoyant, F. Giovannelli, F. Delorme, and A. Stepanov, *Semicond. Sci. Technol.* **30**, 075004 (2015).
[14] P. H. Kasai, *Phys. Rev.* **130**, 989 (1963).
[15] L. S. Vlasenko and G. D. Watkins, *Phys. Rev. B* **72**, 035203 (2005).
[16] Y. Hu and H.-J. Chen, *J. Nanopart. Res.* **10**, 401 (2008).
[17] L. S. Vlasenko, *Appl. Magn. Reson.* **39**, 103 (2010).
[18] J. E. Stehr, S. L. Chen, S. Filippov, M. Devika, N. Koteeswara Reddy, C. W. Tu, W. M. Chen, and I. A. Buyanova, *Nanotechnology* **24**, 015701 (2013).
[19] X. J. Wang, I. A. Buyanova, W. M. Chen, C. J. Pan, C. W. Tu, *J. Appl. Phys.* **103**, 023712 (2008).
[20] X. J. Wang, W. M. Chen, F. Ren, S. Pearton, and I. A. Buyanova, *J. Appl. Phys.* **111**, 043520 (2012).
[21] P. Jakes and E. Erdem, *Phys. Status Solidi* RRL **5**, 56 (2011).
[22] H. Kaftelen, K. Ocakoglu, R. Thomann, S. Tu, S. Weber, and E. Erdem, *Phys. Rev. B* **86**, 014113 (2012).
[23] S. K. S. Parashar, B. S. Murty, S. Repp, S. Weber, and E. Erdem, J. Appl. Phys. 111, 113712 (2012).